Using Pair Approximations to Predict Takeover Dynamics in Spatially Structured Populations

Joshua L. Payne
Dept. of Computer Science
University of Vermont
Burlington, VT 05405
1-802-656-9116
Joshua.Payne@uvm.edu

Margaret J. Eppstein
Dept. of Computer Science
University of Vermont
Burlington, VT 05405
1-802-656-1918
Maggie.Eppstein@uvm.edu

ABSTRACT
The topological properties of a network directly impact the flow of information through a system. For example, in natural populations, the network of inter-individual contacts affects the rate of flow of infectious disease. Similarly, in evolutionary systems, the topological properties of the underlying population structure affect the rate of flow of genetic information, and thus affect selective pressure. One commonly employed method for quantifying the influence of the population structure on selective pressure is through the analysis of takeover time. In this study, we reformulate takeover time analysis in terms of the well-known Susceptible-Infectious-Susceptible (SIS) model of disease spread. We then adapt an analytical technique, called the pair approximation, to provide a general model of takeover dynamics. We compare the results of this model to simulation data on a total of six regular population structures and discuss the strengths and limitations of the approximation.

Categories and Subject Descriptors
I.2.8 Artificial Intelligence [**Problem Solving, Control Methods and Search**]: *Heuristic Methods*

General Terms
Algorithms, Design, Experimentation, Performance

Keywords
Pair Approximation, Takeover Time, Networks, Selective Pressure, Spatial Structure

1. INTRODUCTION
Network topology plays a large role in governing the flow of information throughout a system. For example, in epidemiological models, the structure of the underlying contact network has a pronounced impact on the rate of flow of infectious disease [8][9][13][15]. One of the most commonly studied models of disease spread is the so-called Susceptible-Infectious-Susceptible (SIS) model. In this simplified formulation of infection dynamics, susceptible individuals (*S*) contract disease from infected individuals (*I*) at a given rate, and after a period of time, recover from the disease, again becoming susceptible. While early SIS models assumed that inter-individual contacts were made at random (*e.g.* see [1]), this mean-field assumption was later relaxed to accommodate more realistic contact networks [8][9][13][15]. One popular technique for modeling the transmission of disease throughout such structured populations is the *pair approximation* [8][9]. This analytical method implicitly models the local structure of the underlying contact network, and has been shown to produce results in better agreement with simulation data than corresponding mean-field formulations, when applied to specific forms of contact networks [9][22][23].

In evolutionary systems, the spatial nature of the underlying contact network (*i.e.* population structure) has also been shown to have a large influence on emergent dynamics (*e.g.* [4][10][18] [25]). For example, the spatial localization of recombination events in evolutionary algorithms has been shown to mitigate selective pressure [5][19][21], relative to panmictic population structures, and thus enhance the exploratory power of evolutionary search [5]. One useful method for quantifying the influence of the underlying population structure on selective pressure is through the analysis of *takeover time* [6]. Takeover time is defined as the expected number of generations until a population consists entirely of copies of the best individual, starting with only one copy of the best individual in the initial population. Higher takeover times suggest lower selective pressure and *vice versa*.

Takeover time analysis and the SIS model of disease spread share many similarities. While the SIS model is concerned with the flow of infectious disease throughout a population of susceptible individuals, takeover time analysis focuses on the spread of advantageous genetic information throughout a population of individuals that do not possess this beneficial trait. Thus, takeover time analysis can be viewed as a simplified form of SIS, where low fitness individuals correspond to the susceptible state and high fitness individuals correspond to the infected state. Despite the clear relationship between these two classes of models, this is the first time, to the best of our knowledge, that this correspondence has been explicitly made. While models of takeover dynamics have been previously derived for several regular population structures (*e.g.* [5][19]), each model has been specifically tailored to deal with the contact network under consideration, and therefore lacks generality. In this brief study, we reformulate takeover time analysis in terms of the SIS model of disease spread, and adapt the pair approximation to model takeover dynamics, providing a more general model. We compare the predictions of this model to

GECCO '07, July 7–11, 2007, London, England, United Kingdom.

simulation data on a total of six regular population structures and show that the pair approximation most accurately estimates takeover dynamics on contact networks that possess a preponderance of spatially-localized clustering, but exhibits increasing bias as the degree and locality of clustering deviate from this.

2. METHODS

2.1 Population Structure as a Graph

While canonical evolutionary algorithms [7] typically allow mating interactions to occur between any pair of individuals, there has been a growing interest in imposing constraints upon the spatial scale of mating interactions [3][4][5][16][18][19][20][21]. Such spatial localization of recombination events has been shown to reduce selective pressure [5][20][21] and enhance the exploratory power of genetic search [5]. The most commonly employed, spatially localized interaction topologies are low-order, regular graphs such as one-dimensional (1D) and two-dimensional (2D) toroidal lattices. In such cellular [5][19][21] (also referred to as graph-based [3]) population structures, mating events are restricted to occur within spatially localized, overlapping neighborhoods.

Representing such spatially-explicit population structures as a graph is straightforward. A graph, $G = (V, E)$, is defined as a nonempty finite set of vertices (V) and a finite set of edges (E) connecting these vertices. Each individual in the population is represented by a vertex $i \in V$, so that $|V| = N$, where N is the population size. An undirected edge $<i, j>$ is added to E for each individual j in the mating neighborhood of individual i, for all $i \in V$. 1D and 2D toroidal lattices thus correspond to low-order regular graphs, wherein each vertex has the same degree (*i.e.* every individual has the same number of individuals in its mating neighborhood) and panmictic population structures correspond to complete graphs (*i.e.* fully connected regular graphs).

2.2 Structural Metrics of Graphs

When quantifying the structural properties of a graph, there are several metrics of potential interest. In this section, we briefly define the structural properties considered in the current study. The first metric, ϕ, captures the degree of clustering [24] in a graph G, stored as an adjacency matrix A, as the ratio of closed triangles to total triplets [8],

$$\phi = \frac{\#triangles}{\#triplets} = \frac{trace(A^3)}{\left\|A^2\right\| - trace(A^2)} \tag{2.2.1}$$

where the superscripts denote matrix exponentiation and $\|A\|$ denotes the sum of all the elements in a matrix A.

The second metric, referred to as *radius* [21], captures the level of dispersion present in an interaction neighborhood of size k centered on a vertex at (x,y). This metric has been shown to largely govern selective pressure in regular population structures, with smaller radii inducing lower selective pressure, and *vice versa*. Formally, this metric is defined as [21],

$$radius = \sqrt{\frac{\sum_{i=1}^{k}(x_i - \bar{x})^2 + \sum_{i=1}^{k}(y_i - \bar{y})^2}{k}} \tag{2.2.2}$$

where

$$\bar{x} = \frac{\sum_{i=1}^{k} x_i}{k}, \quad \bar{y} = \frac{\sum_{i=1}^{k} y_i}{k} \tag{2.2.3}$$

2.3 Population Structures

In this study, we investigate takeover dynamics on a total of six population structures, each based on a square 2D toroidal lattice, but with different local interaction neighborhoods. The relevant topological characteristics of each population structure are provided in Table 1. The local neighborhood structures considered varied in both the number and the spatial locality of the individuals they contain, resulting in different clustering characteristics of the graphs as a whole. The naming conventions and corresponding schematic diagrams of these population structures are provided in Table 2. For convenience, we numbered these population structures according to their proportion of spatially localized clustering (C). For example, the neighborhood referred to as *C0* (Table 2), which is more commonly known as the Von Neumann neighborhood, exhibits no clustering, the neighborhood referred to as *C1* (Table 2, a.k.a. a Moore neighborhood) exhibits local clustering only, while the neighborhood referred to as *C5* (Table 2) exhibits the highest proportion of non-local clustering (among vertices that are spatially distant to the center of the neighborhood).

2.4 Takeover Time

Consider a population with only two levels of fitness; *i.e.* let $\Lambda_i(t)$ be the fitness value of vertex $i \in V$ at time t, where $\Lambda_i(t) \in \{0, 1\}$ and 1 is more fit than 0. In the initial population, $\Lambda_i(0) = 1$ for exactly one $i \in V$ and $\Lambda_j(0) = 0 \ \forall \ j \neq i \in V$. Let N_t denote the number of nodes with value 1 at time t:

$$N_t = \sum_{\forall i \in V} \Lambda_i(t) \tag{2.4.1}$$

Following [19], we define the takeover time $T = \min\{t \mid N_t = |V|\}$ to be the minimum number of generations such that the most fit individual fully saturates the entire population. Typically, analyses of takeover time assume that N_t can never decrease. That is, once a vertex takes on the value 1, it never changes. However, this nonextinction assumption [20] can be relaxed by allowing vertices of value 1 to revert back to 0 with some probability g. This extinction probability is analogous to mutation, where genetic information is occasionally lost, or to recovery from infection in models of disease spread, where infected individuals either recover and become immune or again become susceptible.

$\hat{E}_i[T]$ is defined as the empirical estimate of the expected takeover

Table 1. Structural metrics of the spatial topologies

Population Structure	*k*	ϕ	*radius*
C0	4	0	0.89
C1	8	0.43	1.16
C2	12	0.46	1.47
C3	8	0.21	1.49
C4	24	0.52	2.00
C5	12	0.28	2.08

Table 2. Naming conventions and schematic diagrams of population structures considered in this study. The numbering convention employed corresponds to the amount and locality of clustering. We also provide the colloquial names of each population structure and the names as they appear in [21]. Each vertex in the interaction neighborhood (black circles) centered around a given vertex (×) shares a link with this center vertex. For clarity, only one representative interaction neighborhood is shown for each type of graph.

Name	a.k.a.	Degree of Local Clustering	Schematic Diagram
C0	Von Neumann, L5	No local clustering	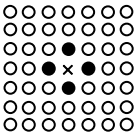
C1	Moore (d = 3), C9	Local clustering only	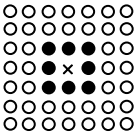
C2	C13		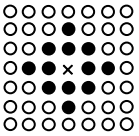
C3	L9		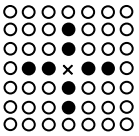
C4	Moore (d = 5)		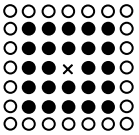
C5	L13	Highest proportion of non-local clustering	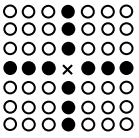

time given that the initial best individual is located in vertex i. Thus, the overall empirically estimated expected takeover time is simply

$$\hat{E}[T] = \frac{1}{|V|} \sum_{\forall i \in V} \hat{E}_i[T] \qquad (2.4.2)$$

assuming that the initial best individual is equally likely to appear in any given node.

2.5 Selection

In this study, we adopt a simple "replace if better" selection mechanism, where nodes are updated synchronously, as follows. For each node $i \in V$, a node j is selected at random with uniform probability from the mating neighborhood of node i, with neighborhood size k_i. Thus, if there are x nodes containing the fittest

value in the mating neighborhood of node i, then the probability of selecting one of them is simply x/k_i. With uptake probability p_{up}, the value of the selected node j then replaced the value of node i if $\Lambda_j(t) > \Lambda_i(t)$. Selective pressure can thus be relaxed by simply decreasing p_{up}.

2.6 The SIS Model and Takeover Time

In the SIS model, a population of N individuals are compartmentalized into two discrete states: susceptible (S) and infected (I). This model evolves according to the following rates

$$S \xrightarrow{p_{up}} I \xrightarrow{g} S \tag{2.6.1}$$

where p_{up} governs the rate at which infection occurs and g governs the rate of recovery from infection. Once a node has recovered, it again becomes susceptible. In a spatially structured population, the transmissibility of disease across a connection is typically assumed to be $\tau = p_{up}/k$ [8][9].

In essence, the SIS model and models of takeover dynamics are one and the same. The susceptible state represents low fitness individuals and the infected state represents high fitness individuals. According to the selection mechanism outlined in section 2.5, transmissibility across a connection occurs at a rate $\tau=p_{up}/k$. That is, there is a $1/k$ chance of a given high fitness individual being selected to spread into a node of degree k, and then, if selected, this individual will spread with probability p_{up}.

While takeover time analysis typically assumes that high fitness individuals never again become low fitness individuals (*i.e.* $g = 0$), this assumption is occasionally relaxed (*e.g.* [20]). Although $g = 0$ in all results reported herein, the formulas presented in the subsequent sections accommodate non-zero g.

2.7 Pair Approximations

Pair approximations, originally borrowed from statistical mechanics [11], are analytical methods for modeling the dynamics of spatially-structured epidemiological systems [8][9]. Instead of modeling the dynamics of the states of *nodes* in a contact network, pair approximations model the dynamics of states of neighboring *pairs* of nodes. By capturing the correlations between pairs of vertices, some aspects of the structure of the interaction topology are implicitly modeled.

The pair approximation works as follows. Consider a population of size N structured on an interaction topology wherein every node has k neighbors, on average. It is important to point out that pair approximations therefore assume that the underlying contact network is regular, or at least possesses a well defined average degree k. Following [8], let $[X]$ denote the number of nodes in state X, $[XY]$ denote the number of pairs of nodes in state XY, and $[XYZ]$ denote the number of triplets in state XYZ, such that XY pairs are always counted once in each direction (*e.g.* $[XY] = [YX]$) and XX pairs are counted twice (*e.g.* $[XX]$ is always even). Pair approximations work by tracking the changes in the numbers of all possible combinations of pairs. Since the interaction topology is regular (*i.e.* k is the same for all nodes), the number of singles can always be recovered from the number of pairs

$$[X] = \frac{1}{k}\sum_{Y}[XY] \tag{2.7.1}$$

Therefore, the only quantities that need to be tracked are pairs. However, one fundamental characteristic of this approach is that the rates of change in the number of pairs depend upon the numbers of configurations larger than pairs. For example, consider a system with two states X and Y, such that nodes in state X spread to adjacent nodes in state Y with transmissibility τ and nodes in state X revert back to state Y at rate g. The rate of change in $[XX]$ is therefore given by

$$\frac{d[XX]}{dt} = -2g[XX] + 2\tau[YX] + 2\tau[XYX] \tag{2.7.2}$$

where the first term on the right hand side of the equation denotes the rate at which $[XX]$ changes to $[XY]$ or $[YX]$, the second term denotes the rate at which $[YX]$ or $[XY]$ change to $[XX]$, and the third term denotes the rate at which either of the neighbors of Y spread into Y, changing $[XYX]$ to $[XXX]$. The rate of change in $[XX]$ therefore depends on the number of triplets of the form $[XYX]$, which is information that is not being maintained. Even if this information was maintained, the rates of change in the number of triplets would similarly depend upon the numbers of even larger configurations. Thus, in order to model the dynamics in terms of the numbers of pairs, the numbers of configurations larger than pairs must be approximated. This is referred to as "closing" the system [22][23].

The most straightforward closure strategy [8] is to assume that such triplets are composed of two independent pairs sharing a common central node. For example, consider $[XYZ]$

$$[XYZ] \approx \frac{(k-1)[XY][YZ]}{\sum_{W}[YW]} = \frac{(k-1)}{k}\frac{[XY][YZ]}{[Y]} \tag{2.7.3}$$

While this assumption closes the system at the level of pairs, it may introduce a significant amount of error. For example, consider the takeover dynamics of a population structured on a regular 2D lattice with 3×3 (Moore) interaction neighborhoods (*i.e.* Table 2, *C1*). In the early stages of the dynamics, only a few of the most fit individuals (*i.e.* 1's) are present in the topology and they are propagating locally through a sea of less fit individuals (*i.e.* 0's). Under this closure assumption, the number of [101] triplets would be approximated by $((k\text{-}1)/k)([10][01]/[0])$. Since both [10] and [01] can be expected to be quite small (and [0] quite large) during the early stages of the takeover dynamics, the approximation of [101] will consequently be very small. However, since the fit individuals are spreading only locally, [101] can actually be expected to be much larger than the number estimated by this approximation. This is especially true if the interaction topology has a preponderance of triangular paths, in which case it is not safe to assume that X and Z are independent of one another in an $[XYZ]$ triplet. Therefore, a more sophisticated closure method is needed.

One such method [8] explicitly takes into consideration the number of triplets in the interaction topology that form triangles. This ratio of closed triangles to total triplets (ϕ, eq. 2.2.1) is then incorporated directly into the closure method as follows,

$$[XYZ] = \frac{(k-1)}{k}\frac{[XY][YZ]}{[Y]}\left((1-\phi) + \frac{\phi N}{k}\frac{[XZ]}{[X][Z]}\right) \tag{2.7.4}$$

Thus, this closure method captures the correlation between nodes at the opposing ends of a triplet in proportion to the ratio of the number of closed triangles to total triplets inherent in the underlying population structure.

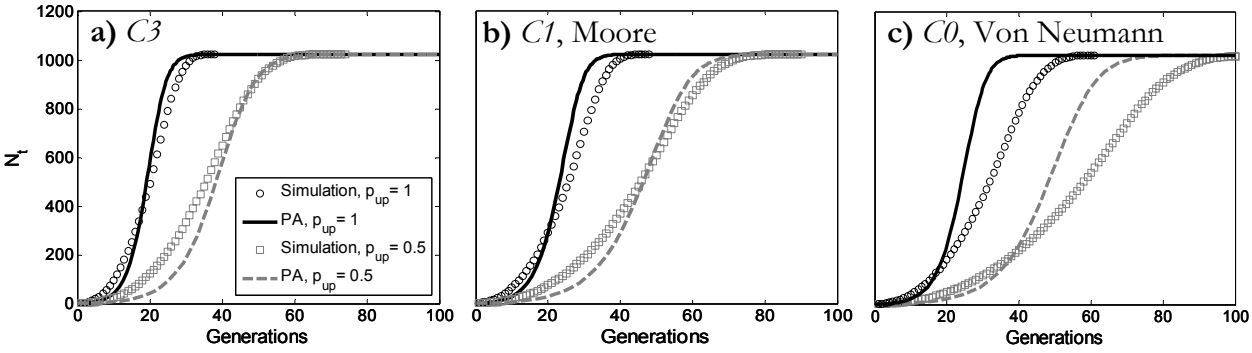

Figure 1. Takeover dynamics observed through direct simulation (o and □ symbols; average of 50 trials) and as predicted by the pair approximation (PA, solid and dashed lines) for p_{up} = 1 (black) and p_{up} = 0.5 (grey), respectively, on the (a) C3, (b) C1, and (c) C0 population structures. The legend and y-axis label apply to all figures.

2.8 Modeling Takeover Dynamics using Pair Approximations

In this section, we develop a pair approximation of takeover dynamics that closely follows the SIS pair approximation proposed in [8]. Our model has only two states, 0 for low fitness individuals and 1 for high fitness individuals, and is parameterized by the population size (N), the average vertex degree (k), the ratio of closed triangles to total triplets (ϕ), the extinction probability (g), and the uptake probability (p_{up}). With only two states, there exist four distinct types of pairs. However, due to symmetry ([01]=[10]), only three differential equations are required:

$$\begin{aligned}\frac{d[00]}{dt} &= -2\tau[001] + 2g[01],\\ \frac{d[01]}{dt} &= \tau([001]-[101]-[01]) + g([11]-[01]),\\ \frac{d[11]}{dt} &= 2\tau([101]+[01]) - 2g[11]\end{aligned} \qquad (2.8.1)$$

where triplets are closed at the level of pairs using equation 2.7.4 and $\tau = p_{up}/k$.

2.9 Experimental Design

The population size was held constant in all experiments at 1024 individuals (*i.e.* $|V|$=1024). For each of the six population structures considered, we performed 50 independent takeover time simulations, starting with the copy of the best individual in a randomly chosen node. Since each of the population structures considered in this study are regular (*i.e.* each individual has the same number of potential mates in its local neighborhood), this random initial placement should not introduce any bias into the experimental design (*i.e.* $E[T] = E_i[T] \forall i \in V$). Further, the 50 independent simulations performed for each population structure should be sufficient to mitigate the stochasticity inherent in the selection policy.

The coupled differential equations of the pair approximation (eq. 2.8.1) were solved *via* numerical integration using the values of k and ϕ outlined in Table 1. For each population structure, we considered $p_{up} \in \{0.5, 1\}$. As previously stated, all experiments reported here were nonextinctive [19][20]; *i.e.*, $g = 0$.

3. RESULTS

Figure 1 depicts the observed takeover dynamics using both the pair approximation and direct simulation on a square 2D lattice with the *C3* (Figure 1a), *C1*, (Figure 1b), and *C0* (Figure 1c) neighborhoods. For the simulation results, we plot the number of nodes containing maximum fitness at time t (N_t), averaged over all 50 independent simulations. All takeover curves are sigmoidal, exhibiting exponential growth followed by saturation. For both the *C3* (Figure 1a) and *C1* (Figure 1b) neighborhoods, the dynamics predicted by the pair approximation are in reasonable agreement with the simulation data. However, for the *C0* neighborhood, the pair approximation estimates a more rapid spread of the high fitness individual than that observed through direct simulation (Figure 1c).

Table 3 displays, for each population structure considered, the times to complete saturation observed through direct simulation and as predicted by the pair approximation. For both p_{up} = 0.5 and p_{up} = 1, the observed saturation time decreased as the spatial locality of the interaction neighborhood decreased, with *C0* exhibiting the longest time to saturation, followed by *C1*, *C2*, etc., with *C5* the most rapid. Figure 2 depicts the absolute error between the time to complete saturation estimated by the pair approximation and observed through direct simulation. The absolute error is quite high for *C0* (*e.g.* Figure 1c), but drops quickly for *C1* through *C3*, and rises again for *C4* through C6. For p = 1, *C0* exhibits the largest absolute error, but for p = 0.5, this trend changes, with C6 exhibiting the largest absolute error overall. In all cases, increasing p_{up} decreased the absolute error, with the smallest amount of change observed using the *C0* and *C1* population structures. Note that the *C2* and *C3* population structures were found to have almost identical saturation times (Table 3) and absolute error (Figure 2).

4. DISCUSSION AND CONCLUSIONS

For all population structures considered herein, the average time to saturation decreased as the degree of clustering among spatially distant vertices increased (*i.e. C0* exhibited the largest saturation time, and *C5* the lowest). This qualitative categorization of the neighborhood structures is directly correlated with the *radius* metric presented in [21] (see Table 2). Population structures with local neighborhoods of large *radii* have been shown to saturate more quickly than those with smaller *radii* in some cases [21]. Our simulation results are in good agreement with this finding. It is worth noting that the nearly identical saturation times of the *C2* and

Table 3. Takeover times as observed through direct simulation (average of 50 trials) and as predicted using the pair approximation (PA) for uptake probabilities p_{up} = 1 and p_{up} = 0.5 on each population structure. The absolute error (in generations) between the observed and predicted takeover times are also provided.

Population Structure	p_{up} = 1			p_{up} = 0.5		
	Simulation	PA	Error	Simulation	PA	Error
C0	55.20	42.88	12.32	99.10	85.75	13.35
C1	42.92	41.27	1.65	78.82	82.68	3.86
C2	35.06	36.92	1.86	63.78	73.81	10.03
C3	34.30	36.21	1.91	62.32	72.43	10.11
C4	26.46	33.69	7.23	48.74	67.37	18.63
C5	26.08	33.87	7.79	48.40	67.75	19.35

C3 population structures were also observed in [21] (referred to therein as C13 and L9, respectively), and that this similarity was captured well using the pair approximation (*e.g.* compare *C2* and *C3* in Table 3 and Figure 2). In all cases, increasing p_{up} decreased the absolute error between the saturation times predicted by the pair approximation and those observed through simulation. Absolute error is relatively insensitive to p_{up} for the Von Neumann (*C0*) and 3×3 Moore (*C1*) neighborhoods (Figure 2), most likely resulting from the regularity and locality inherent in these interaction neighborhoods.

The results of this study demonstrate that the accuracy of the pair approximation presented in section 2.8 depends heavily upon the amount and locality of clustering in the underlying population structure. The accuracy of the pair approximation was found to be the highest for population structures possessing a large proportion of spatially localized clustering in the mating neighborhood (*i.e. C1*, *C2*, and *C3*), and for these graph structures the approximation is a fast way to estimate takeover dynamics for arbitrary p_{up} and g on graphs of various sizes. In contrast, when the interaction neighborhood had no clustering (*i.e. C0*), or a large proportion of clustering among spatially distant vertices (*i.e. C4* and *C5*), the pair approximation was found to perform poorly. These limitations should be taken into account when applying the pair approximation to takeover times in evolutionary algorithms as well as in epidemiological models.

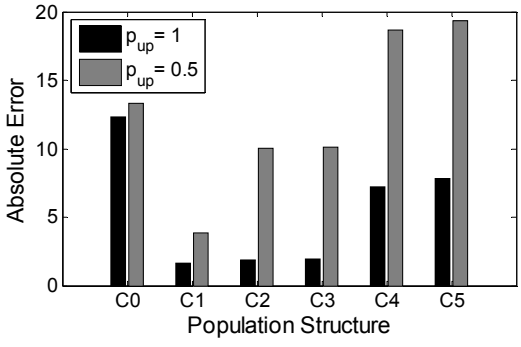

Figure 2. Absolute error (in generations) between takeover times observed through direct simulation (average of 50 trials) and predicted by the pair approximation on all population structures for p_{up} = 1 (black) and p_{up} = 0.5 (grey). Data corresponds to absolute errors presented in Table 3.

To understand the degradation in accuracy observed using population structures possessing no clustering, consider the Von Neumann neighborhood (*C0*). Since $\phi = 0$, there are no closed triangles present in the contact network. The pair approximation thus assumes that there are no correlations between distant ends of triplets and the closure method of equation 2.7.4 reduces to equation 2.7.3. While it is certainly correct to assume that there are no closed triangles in this population structure, there are a large number of closed quadruplets, and these can significantly impact the emergent dynamics. Making the assumption that the distant ends of a triplet are completely uncorrelated with one another therefore leads to a significant amount of error. For instance, consider an *ijkl* quadruplet. While the state of node *k* cannot directly affect the state of node *i*, it can have an affect on *l*, which in turn may affect *i*. By ignoring quadruplet correlations and assuming no correlation between the distant ends of triplets, the pair approximation treats the *C0* population structure as if it were a random graph (*e.g.* [14]) of average degree *k*. This explains the more rapid saturation predicted by the pair approximation than that observed through direct simulation (Figure 1c). While the pair approximation can be altered to deal with closed quadruplets [12], or other spatial configurations [22][23], the resulting models become more cumbersome (*e.g.* see [12]) and far less general.

In the case of population structures possessing a large proportion of clustering among spatially distant vertices in their local mating neighborhoods, the degradation in accuracy can be best understood by considering the *C5* topology. Since the pair approximation does not take into account the spatial distance of links between individuals, this approximation assumes that all of the clustering occurs between purely spatially local vertices. The pair approximation is thus unable to predict the effects of information spread between non-local vertices, which dramatically impacts the emergent dynamics (*e.g.* [18]), and the resulting predictions are therefore much slower than that observed through direct simulation. To the best of our knowledge, a general analytical model that captures the spatial scale of clustered interactions has not yet been developed.

Thus, the pair approximation presented in section 2.8 can be viewed as a generalized model of takeover dynamics, applicable to a specific class of population structures; in particular, those exhibiting primarily localized clustering. While the naming conventions of the population structures considered herein (Table 2), based on a qualitative assessment of the spatial locality of clustered vertices, allowed for a verbal classification of each interaction topology, it

would be useful to explicitly quantify this metric. For example, the global degree of clustering (ϕ) could be altered to account for the proportion of clustered nodes found at various spatial distances. This may allow for a more concrete classification of the regular spatial topologies in which takeover dynamics can be accurately modeled using the pair approximation.

We posit that the derivation of a generalized analytical model of takeover dynamics for all population structures is precluded by the heterogeneity inherent in some of the non-regular population structures of recent interest (*e.g.* small-world [24] and scale-free [2]). These contact networks have large variance in their underlying topological properties and it does not seem likely that a model of takeover dynamics applicable to lattice-based topologies, which have a well-defined average degree, would be equally applicable to scale-free topologies, which possess a degree distribution following a power law. While the derivation of a generalized model of takeover *dynamics* may be out of reach, a recent study [17] has demonstrated that it may be possible to predict the expected takeover *times* on disparate topologies, using only a few readily computed metrics of the underlying population structure.

5. Acknowledgements

This work was supported in part by a graduate research assistantship and a Pilot Award funded by DOE-FG02-00ER45828 awarded by the US Department of Energy through its EPSCoR program. We would like to thank Dr. Peter Dodds for helpful discussions regarding the use of pair approximations.

6. References

[1] Anderson, R.M., & May, R.M. *Infectious Diseases of Humans*. Oxford University Press, 1995.

[2] Barabàsi, A.L. & Albert, R. Emergence of scaling in random networks. *Science*, 286 (1999), 509-512.

[3] Bryden, K.M., Ashlock, D., Corns S., Wilson, S. Graph based evolutionary algorithms. *IEEE Transactions on Evolutionary Computation*, 10, 5 (2005), 550-567.

[4] Giacobini, M., Tomassini, M., & Tettamanzi, A. Takeover time curves in random and small-world structured populations. In *Proc. Genetic and Evolutionary Computation Conference*. ACM Press, New York, NY, 2005, 1333-1340.

[5] Giacobini, M., Tomassini, M., Tettamanzi, A., & Alba, E. Selection intensity in cellular evolutionary algorithms for regular lattices. *IEEE Transactions on Evolutionary Computation*, 9, 5 (2005), 489-505.

[6] Goldberg, D.E., & Deb, K. A comparative analysis of selection schemes used in genetic algorithms. In *Proc. Foundations of Genetic Algorithms*. Morgan-Kauffman, San Mateo, CA, 1991, 69-93.

[7] Holland, J. *Adaptation in Natural and Artificial Systems*. MIT Press, Cambridge, MA, 1992.

[8] Keeling, M.J. The effects of local spatial structure on epidemiological invasions. *Proc. R. Soc. Lond. B*, 266 (1999), 859-867.

[9] Keeling, M.J., & Eames, K.T.D. Networks and epidemic models. *J. R. Soc. Interface*, 2 (2005), 295-307.

[10] Kerr, B., Riley, M.A., Feldman, M.W., & Bohannan, B.J.M. Local dispersal promotes biodiversity in a real life game of rock-paper-scissors. *Nature*, 418 (2002), 171-174.

[11] Matsuda, H., Ogita, N., Sasaki, A., & Soto, K. Statistical mechanics of population: the lattice Lotka-Volterra model. *Prog. Theor. Phys.* 88 (1992), 1035-1049.

[12] Morris, A.J. Representing spatial interactions in simple ecological models. *PhD Thesis.* University of Warwick, UK.

[13] Newman, M.E.J. Spread of epidemic disease on networks. *Phys. Rev. E*, 66 (2002), 016128.

[14] Newman, M.E.J. The structure and function of complex networks. *SIAM Review*, 45 (2003), 167-256.

[15] Pastor-Satorras, R. & Vespignani, A. Epidemic spreading in scale-free networks. *Physical Review Letters*, 86, 14 (2001), 3200.

[16] Payne, J.L., & Eppstein, M.J. Emergent mating topologies in spatially structured genetic algorithms. In *Proceedings of the Genetic and Evolutionary Computation Conference*. ACM Press, New York, NY, 2006, 207-214.

[17] Payne, J.L., & Eppstein, M.J. Takeover times on scale-free topologies. In *Proceedings of the Genetic and Evolutionary Computation Conference*, 2007, *to appear*.

[18] Payne, J.L., Eppstein, M.J., & Goodnight, C.J. Sensitivity of self-organized speciation to long-distance dispersal. *Proceedings of the IEEE Symposium on Artificial Life*, 2007, 1-7.

[19] Rudolph, G. On takeover times in spatially structured populations: array and ring. In *Proc. 2nd Asia-Pacific Conference on Genetic Algorithms and Applications*. Global-Link Publishing Company, Hong Kong, 2000, 144-151.

[20] Rudolph, G. Takeover times of noisy non-generational selection rules that undo extinction. In *Proc. 5th International Conference on Artificial Neural Networks and Genetic Algorithms*. Springer-Verlag, Heidelberg, 2001, 268-271.

[21] Sarma, J. & De Jong, K. An analysis of the effect of the neighborhood size and shape on local selection algorithms. In *Proc. Parallel Problem Solving from Nature Conference*. Springer-Verlag, Heidelberg, 1996, 236-244.

[22] Satō, K., & Iwasa, Y. Pair approximations for lattice-based ecological models. In *The Geometry of Ecological Interactions: Simplifying Spatial Complexity.* Cambridge University Press, 2000, 341-358.

[23] Van Baalen, M. Pair approximations for different spatial geometries. In *The Geometry of Ecological Interactions: Simplifying Spatial Complexity.* Cambridge University Press, 2000, 359-387.

[24] Watts, D.J., & Strogatz, S.H. Collective dynamics of 'small-world' networks. *Nature*, 393 (1998), 440-442.

[25] Werfel, J. & Bar-Yam, Y. The evolution of reproductive restraint through social communication. *PNAS*, 101, 30 (2004), 11019-11024.